

Supporting Information

for

2D MOFs-based artificial light-harvesting system with chloroplast bionic structure for photochemical catalysis

**Zhong Wei Jiang^a, Ting Ting Zhao^a, Shu Jun Zhen^a, Chun Mei Li^b, Yuan Fang
Li^{a*}, and Cheng Zhi Huang^{a, b *}**

^a Key Laboratory of Luminescence Analysis and Molecular Sensing, Ministry of Education, College of Chemistry and Chemical Engineering, Southwest University, Chongqing 400715, P. R. China.

^b Key Laboratory of Luminescence and Real-Time Analysis System, Chongqing Science and Technology Bureau, College of Pharmaceutical Sciences, Southwest University, Chongqing 400715, P. R. China.

Experimental Section

1. Chemicals.

Yb(NO₃)₃·5H₂O, 9,10-diphenylanthracene (DPA), 1,5-dihydroxynaphthalene (1,5-DHN), Sodium dodecyl sulfate (SDS), methylene blue (MB), biphenyl, chloroform-d, and Rose Bengal (RB) were purchased from Aladdin (Shanghai, China). Tetrakis(4-carboxyphenyl) porphyrin (H₂TCPP) was obtained from Frontier Scientific (Logan, Utah, USA). Ethanol, N,N-dimethylacetamide (DMA), dichloromethane (DCM), sulfuric acid (H₂SO₄), hydrochloric acid (HCl), nitric acid (HNO₃), and trifluoroacetic acid (TFA) were purchased from Chuandong Chemical Co., Ltd. (Chongqing, China). Dihydroartemisinic acid was obtained from Staherb Natural Ingredients Co., Ltd. (Changsha, China). trimethylphosphine oxide (TMPO) was obtained from J&K scientific Ltd (Beijing, China). All chemicals were used as received without further purification. Ultrapure water (18.2 MΩ) was obtained from the Milli-Q system.

2. Material synthesis.

Synthesis of 2D Yb-TCPP nanosheets: The 2D Yb-TCPP nanosheets were synthesized according to our previous report with some modification.¹ Firstly, Yb(NO₃)₃·5H₂O (0.09 mmol, 40.4 mg) and 0.03 mmol H₂TCPP (23.7mg) were dissolved in 9 mL DMA, respectively. Then, 400 μL Yb(NO₃)₃ solution and 400 μL H₂TCPP solution were added into a 3 mL Pyrex vial, and the mixture was further diluted to 1 mL with DMA. After that, the capped vials were heated for 10 minutes under microwave irradiation in a household microwave oven (M1-L213B, Midea Co., Ltd., China) with medium low power (about 231W). After cooling down to room temperature, the resulting nanosheets were washed twice with DMA and ethanol

repectively, and then collected by centrifuge at 15,000 r.p.m for 10 min. Finally, the obtained 2D Yb-TCPP nanosheets were redispersed in ethanol.

Synthesis of 2D MB/Yb-TCPP-SO₄ nanosheets: 5 mL 2D Yb-TCPP nanosheets suspension (1mg/mL) was added into a 15 mL EP tube. Then, 1 mL SDS aqueous solution (20mg/mL) was rapidly poured into 2D Yb-TCPP nanosheets suspension under ultrasonication at room temperature. After further ultrasonic reaction for 10 minutes, 1 mL MB aqueous solution (1mg/mL) was rapidly added into the suspension under ultrasonication. After ultrasonic reaction for another 10 minutes, the suspension was shaken at 25 °C for 1 hour in an oscillator with the speed of 150 r.p.m. Finally, the obtained crude product was washed with ethanol until the supernatant becomes colorless.

Acid treatment: 5 mg as-synthesized 2D MB/Yb-TCPP-SO₄ nanosheets were immersed in 5 mL H₂SO₄ with various concentrations (0.001M, 0.002M, 0.005M and 0.01 M) for 24 h. The solution was then removed by freeze-drying, followed by vacuum drying at 60 °C. For treatment with other acid, such as HNO₃, HCl and TFA, the similar procedure was carried with a constant concentration of 0.01 M.

³¹P MAS NMR Characterizations of 2D MB/Yb-TCPP-HSO₄ nanosheets:

According to previous reports,²⁻⁵ about 100 mg of each 2D MB/Yb-TCPP-HSO₄ nanosheets were placed in a heat-resisting glass bottle. Firstly, the sample was activated under vacuum at 120 °C for 24h, and 3.0 mL of 0.2 M trimethylphosphine oxide (TMPO) in dichloromethane was then added to the sample cell. After thoroughly mixing the TMPO solution and the 2D MB/Yb-TCPP-HSO₄ nanosheets under

ultrasound, the dichloromethane was removed under vacuum, first at room temperature for 24 h and then at 50 °C for 8 h. The obtained sample was then used for ^{31}P MAS NMR Characterizations. The solid-state nuclear magnetic resonance (SSNMR) spectra were acquired on a Bruker Avance-600MHz NMR spectrometer using a standard Bruker double resonance magic angle-spinning (MAS) probe.

3. Detection of $^1\text{O}_2$ Generation

Chemical capture: Typically, 1 mL of oxygen saturated acetonitrile/ H_2O (5:1) solution containing 9,10-diphenylanthracene (DPA) and different photocatalytic system (2D Yb-TCPP nanosheets, MB, Yb-TCPP+MB, 2D MB/Yb-TCPP- SO_4 nanosheets, and 2D MB/Yb-TCPP- HSO_4 nanosheets) were irradiated with a 300 W Xe lamp (CEL-HXF300, Beijing, China Education Au-light Co., Ltd.) equipped with a 400 nm cut-off filter. The absorption spectra of the samples at different reaction time were performed on UV-vis spectrophotometer.

Detection of $^1\text{O}_2$ by ESR: 2,2,6,6-Tetramethyl-4-piperidone (4-oxo-TMP) was used as a probe to spin trap $^1\text{O}_2$ and afford stable 4-oxo-2,2,6,6-tetramethyl-1-piperidinyloxy (4-oxo-TEMPO), which can be detected via electron spin resonance (ESR) spectroscopy. The ESR spectra of 2D MB/Yb-TCPP- SO_4 nanosheets and 2D MB/Yb-TCPP- HSO_4 nanosheets were obtained with light irradiation. Meanwhile, 2D Yb-TCPP nanosheets, MB and Yb-TCPP+MB were set as the control group.

Evaluation of the $^1\text{O}_2$ quantum yield by detecting its emission: The $^1\text{O}_2$ emission signal around 1270 nm was recorded by Fluorolog-3 (Horiba, Japan) spectrometer under an excitation of 532 nm. RB was used as the standard photosensitizer ($\Phi_{\text{RB}} = 0.86$, in ethanol). The absorptions of RB and photocatalyst at 532 nm were adjusted to

~0.2 OD. The $^1\text{O}_2$ quantum yield of photocatalyst were calculated by comparing the luminescence intensity toward that of RB. In detail, $\Phi_{\text{photocatalyst}} = \Phi_{\text{RB}} (I_{\text{photocatalyst}}/I_{\text{RB}})$, where $I_{\text{photocatalyst}}$ and I_{RB} mean the PL peak areas of $^1\text{O}_2$ produced by photocatalyst and RB, respectively.

4. Photocatalytic oxidation of dihydroartemisinic acid to artemisinin.

The photocatalytic experiment was carried out according to the previous report with some modification.^{6, 7} Typically, dihydroartemisinic acid (25 mg, 0.106 mmol) and photocatalyst (1 mg) were dispersed in DCM (7 mL), and slowly bubbled with O_2 under the irradiation of 300-W Xe lamp at 0 °C for 3 hours. After removal of DCM via rotary evaporation, the conversion and yield of artemisinin was measured by $^1\text{H-NMR}$ in CDCl_3 using biphenyl (16.3 mg, 0.106 mmol) as an internal standard. Moreover, 2D Yb-TCPP nanosheets, MB and Yb-TCPP+MB were set as the control group.

5. Characterization.

The household microwave oven (M1-L213B, Midea Co., Ltd., China) was used to prepare 2D Yb-TCPP nanosheets. The nano particle size and zeta potential meter (ZEN3600, Malvern) was used to measure the change of zeta potential. The morphology of the as-prepared 2D ALHSs was characterized by an S-4800 scanning electron microscope (SEM) (Hitachi, Japan). Transmission electron microscopy (TEM) images were taken on FEI Tecnai G2 F20 TEM instrument (FEI, America). Atomic force microscopy (AFM) images were obtained on a commercial atomic force microscope instrument (Dimension ICON, Bruker, USA). Powder X-ray diffraction (XRD) patterns were recorded on D8 ADVANCE X-ray diffractometer (Bruker, USA), using $\text{Cu K}\alpha$ radiation ($\lambda = 1.5406 \text{ \AA}$). The BET surface area was determined by N_2

adsorption–desorption isotherms obtained at 77 K on ASAP 2020, USA. The 300E electron spin resonance (ESR) spectrometer (Bruker, Germany) was employed to record the ESR spectra at room temperature. Thermogravimetry analysis (TGA) was conducted on a Q600 (TA Instruments, USA) thermogravimetric analyzer. The infrared spectra of the materials were recorded by an IR Prestige-21 (Shimadzu, Japan) instrument in the range of 500–4000 cm^{-1} using the KBr pellet technique. LabRAMHR800 spectrometer excited at 532 nm (Horiba Jobin-Yvon, France) was used to record Raman spectra. ^{31}P MAS NMR characterizations was recorded on a Bruker AVANCE III 600MHz NMR spectrometer (Bruker, Germany) using a standard Bruker double resonance magic angle-spinning (MAS) probe. Uv–Vis spectra and diffuse reflection spectra were recorded with a U-3010 spectrophotometer (Hitachi, Japan). The F-4600 (Hitachi, Japan) and Fluorolog-3 (Horiba, Japan) were used to record the fluorescence spectra and near infrared emission spectra of $^1\text{O}_2$, respectively.

Figures and Tables.

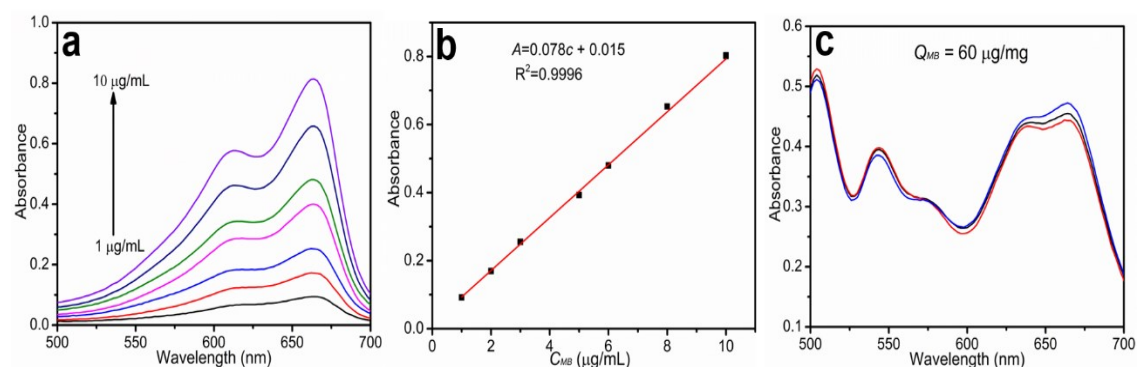


Fig. S1. (a) The UV-vis spectra of MB with different concentration; (b) the corresponding standard curve of MB; and (c) the UV-vis spectra of 2D MB/Yb-TCPP- SO_4 after disintegrating by using NaOH (including three groups of parallel samples).

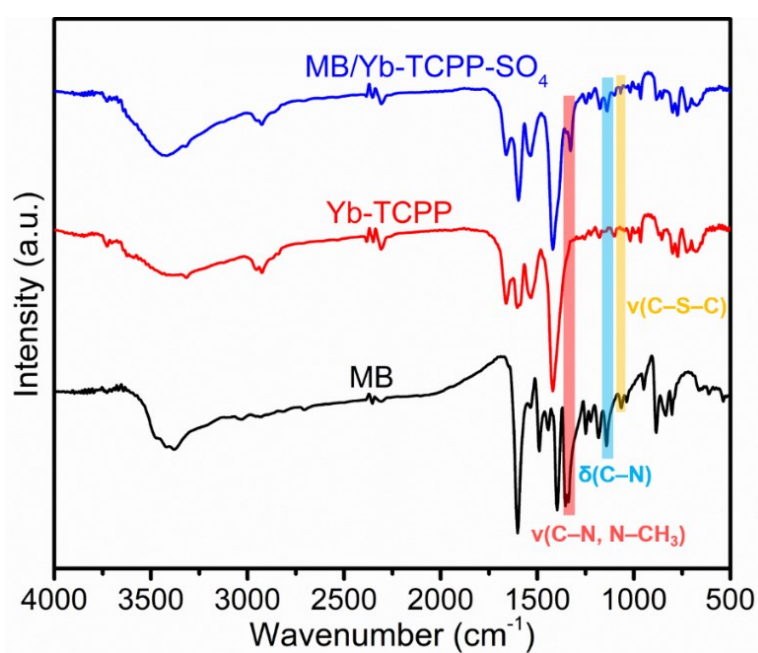


Fig. S2. The infrared spectra of MB, 2D Yb-TCPP nanosheets and 2D MB/Yb-TCPP- SO_4 nanosheet.

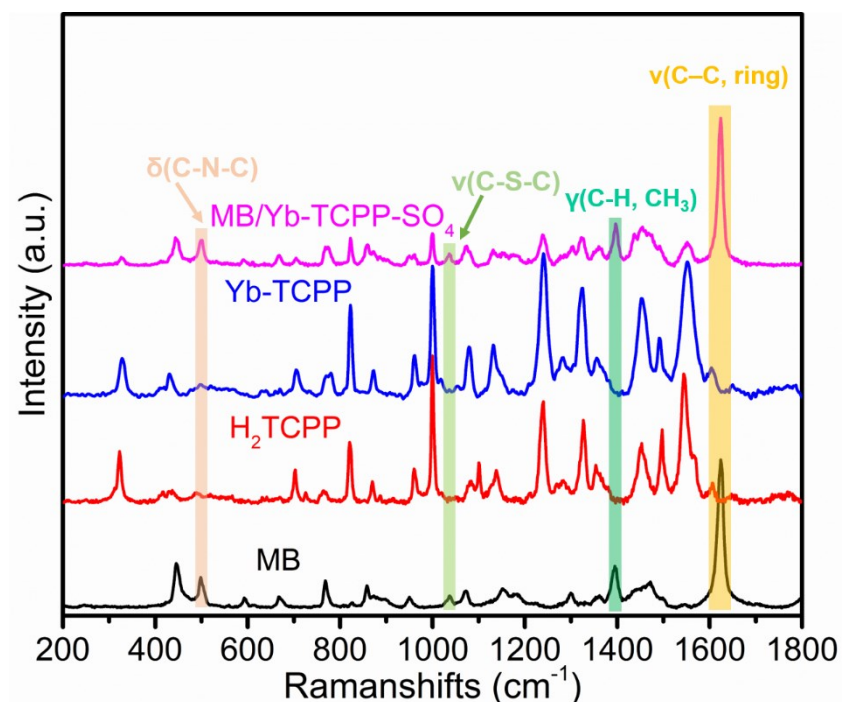


Fig. S3. The Raman spectra of MB, H₂TCPP, 2D Yb-TCPP nanosheets and 2D MB/Yb-TCPP-SO₄ nanosheets.

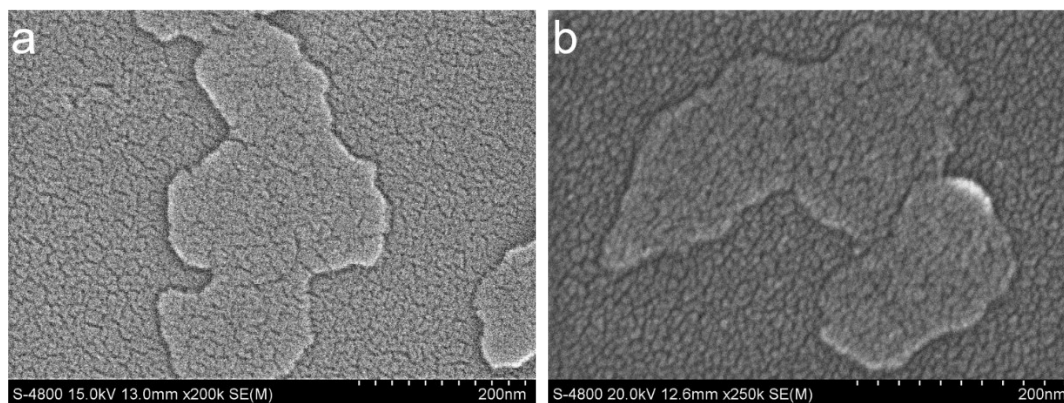


Fig. S4. The SEM images of as-synthesized 2D Yb-TCPP nanosheets (a) and MB/Yb-TCPP-SO₄ nanosheets (b).

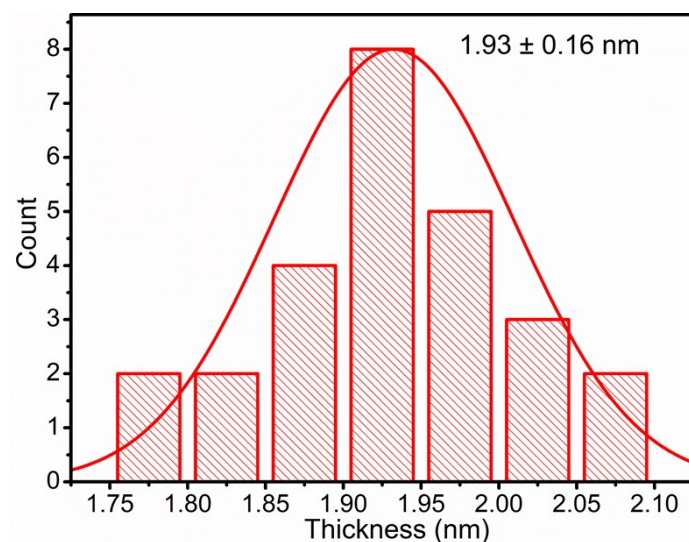


Fig. S5. Thickness distribution histogram of 2D MB/Yb-TCPP-SO₄ nanosheets measured by AFM.

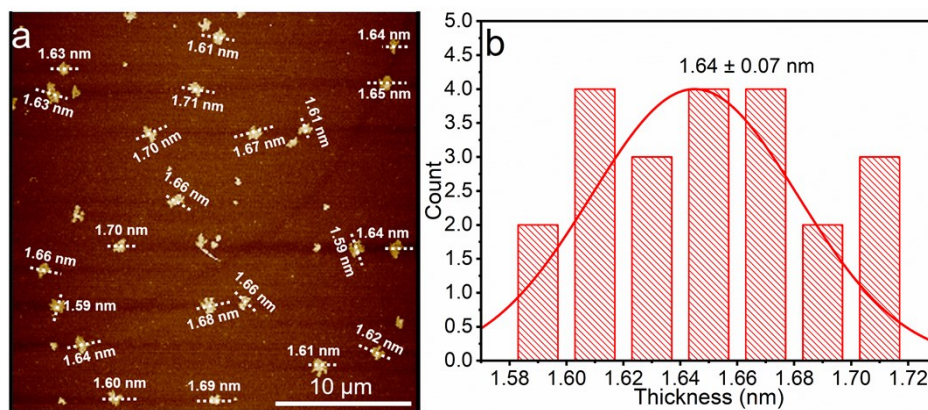


Fig. S6 The AFM image and corresponding thickness distribution histogram of as-synthesized 2D Yb-TCPP nanosheets.

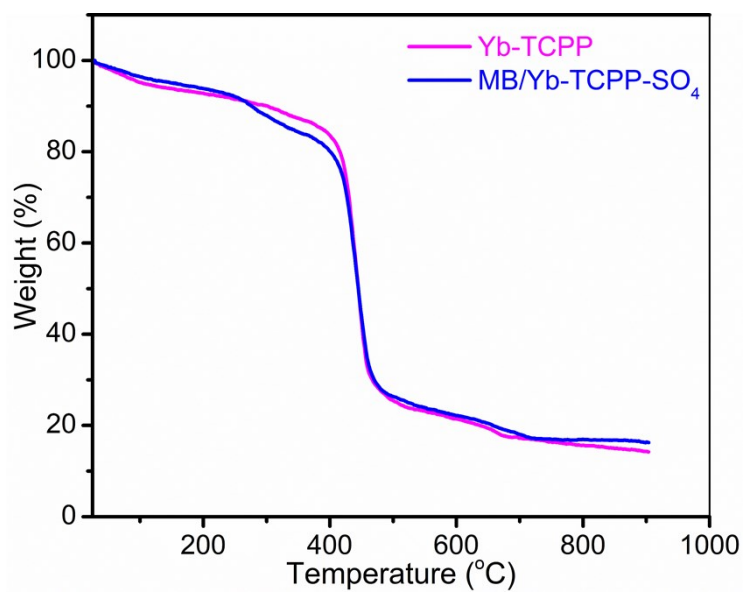


Fig. S7. TGA curves of 2D Yb-TCPP nanosheets and 2D MB/Yb-TCPP-SO₄ nanosheets measured in air atmosphere with a temperature ramp of 10 °C min⁻¹.

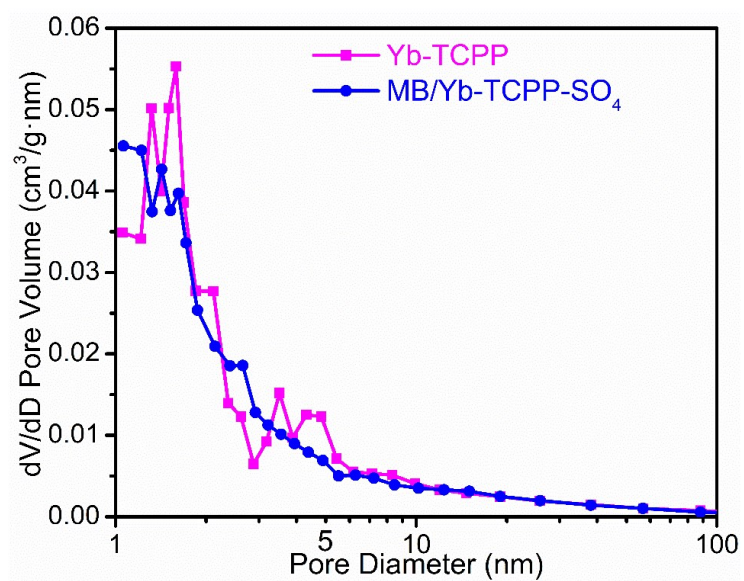


Fig. S8. Pore size distribution profiles of 2D Yb-TCPP nanosheets and 2D MB/Yb-TCPP-SO₄ nanosheets.

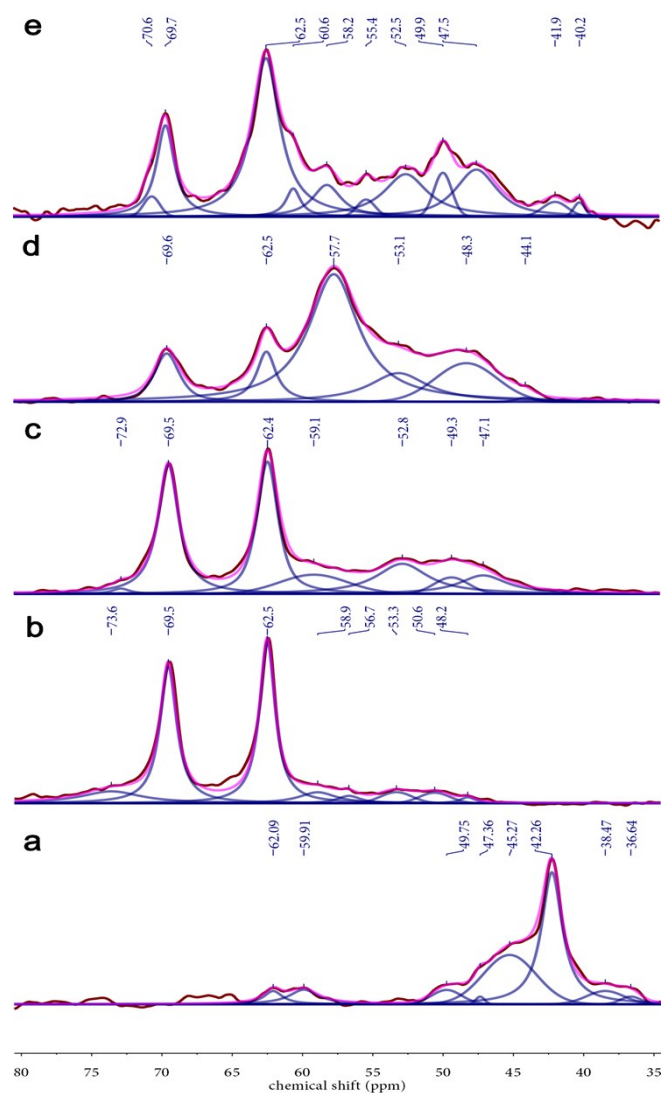


Fig. S9. ^{31}P MAS solid-state NMR spectra of TMPO loaded on MB/Yb-TCPP- SO_4 (a), MB/Yb-TCPP- HSO_4 -0.005- H_2SO_4 (b), MB/Yb-TCPP- HSO_4 -0.01- HNO_3 (c), MB/Yb-TCPP- HSO_4 -0.01- HCl (d) and MB/Yb-TCPP- HSO_4 -0.01- TFA (e). Experimental spectra are shown in maroon, deconvoluted peaks in navy, and the sum of the deconvoluted peaks in magenta.

Trimethylphosphine oxide (TMPO) was chosen as probe to interact with Brønsted acid site via the lone pairs on its oxygen atom. The ^{31}P NMR chemical shift of TMPO molecules adsorbed on Brønsted acid sites is linear with strength of the acid site, where a higher ^{31}P chemical shift corresponds to a stronger acid site.²⁻⁵

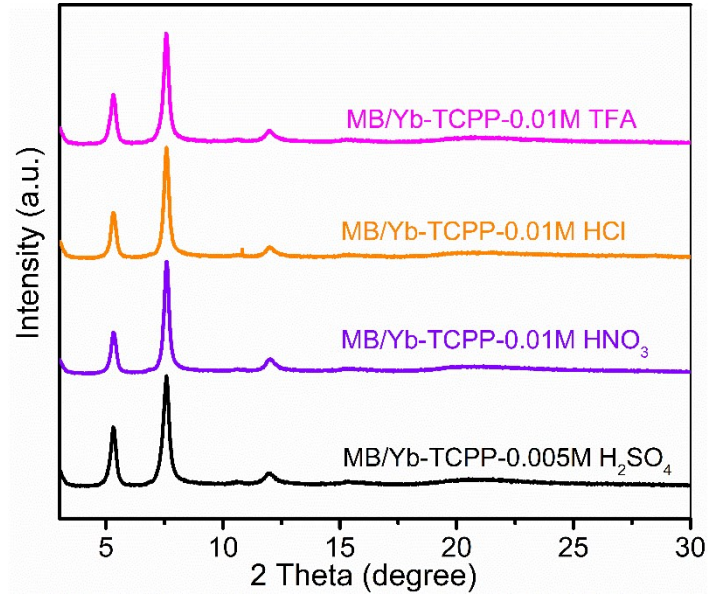


Fig. S10. PXRD patterns of 2D MB/Yb-TCPP-SO₄ nanosheets after soaking in H₂SO₄ (0.005M), HNO₃ (0.01M), HCl (0.01M) and TFA (0.01M), respectively.

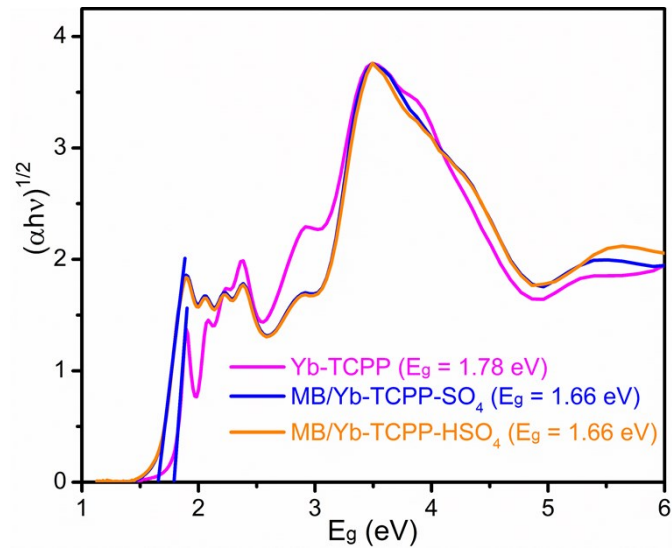


Fig. S11. Tauc plot of 2D Yb-TCPP nanosheets, 2D MB/Yb-TCPP-SO₄ nanosheets and 2D MB/Yb-TCPP-HSO₄ nanosheets. Tauc plot $(\alpha h\nu)^{1/2}$ vs. $(h\nu)$, where α is absorbance.

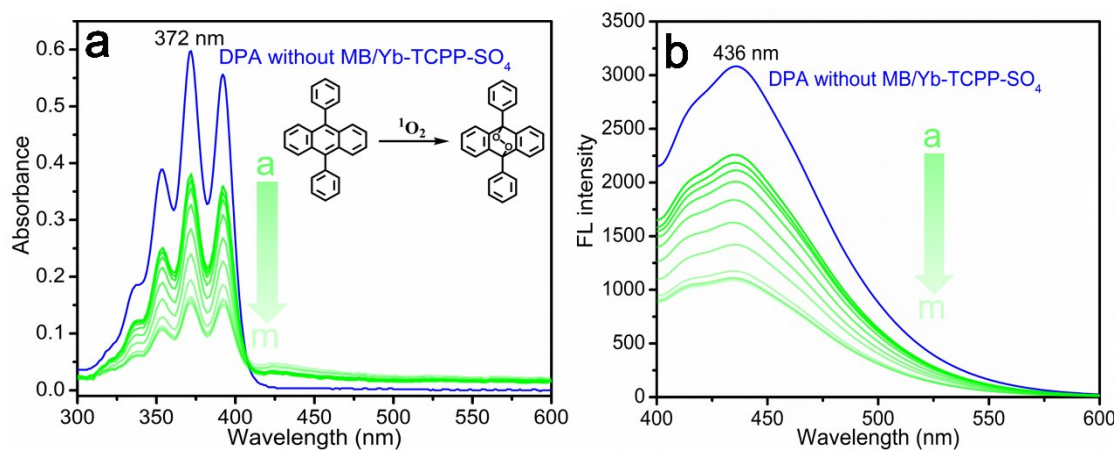


Fig. S12. UV-vis (a) and fluorescence spectra (b) of DPA (20 $\mu\text{g/mL}$) upon light irradiation in the presence of 2D MB/Yb-TCPP-SO₄ nanosheets (2.5 $\mu\text{g/mL}$) with different MB load amount. All the above reactions were carried out in acetonitrile/H₂O (5:1) solution under a 300-W Xe lamp irradiation for 5 min equipped with a 400 nm cut-off filter.

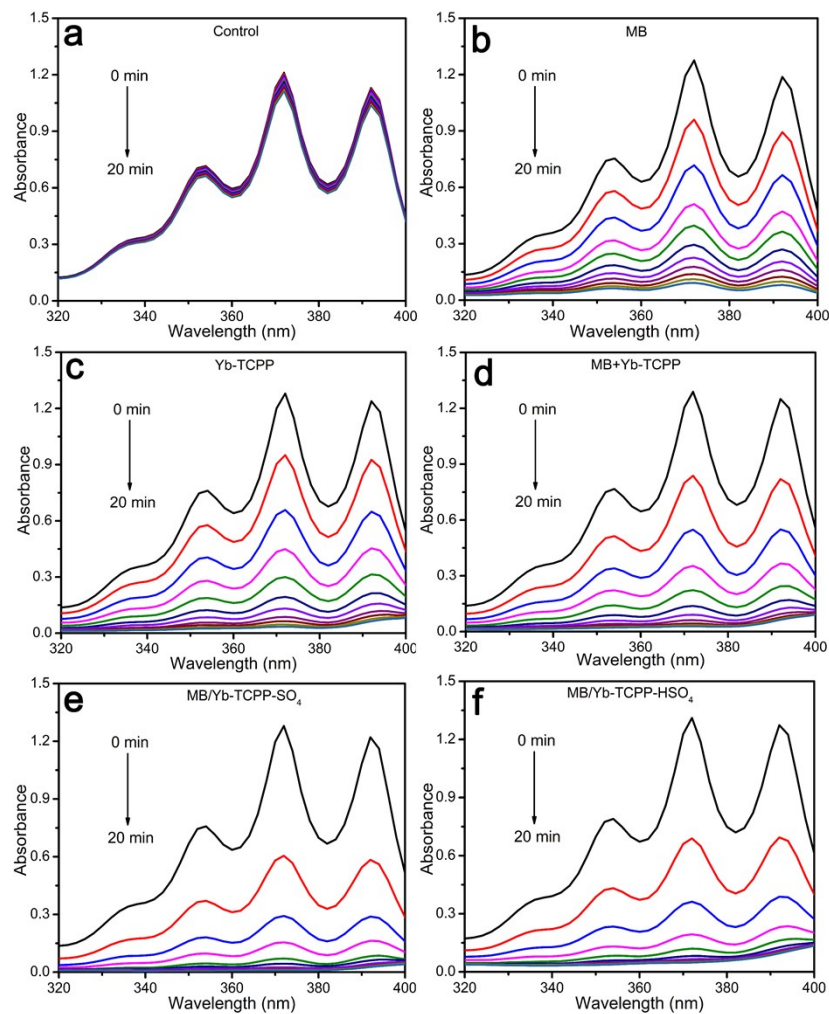


Fig. S13. Time course of absorption spectra of DPA (40 $\mu\text{g/mL}$) upon visible-light irradiation in different reaction systems. (a) control, (b) MB+DPA, (c) 2D Yb-TCPP nanosheets +DPA, (d) MB+Yb-TCPP+DPA, (e) 2D MB/Yb-TCPP-SO₄ nanosheets +DPA, (f) 2D MB/Yb-TCPP-HSO₄ nanosheets+DPA, respectively. All the above reactions were carried out in acetonitrile/H₂O (5:1) solution under a 300 W Xe lamp irradiation equipped with a 400 nm cut-off filter, and the spectra were recorded every 2 minutes.

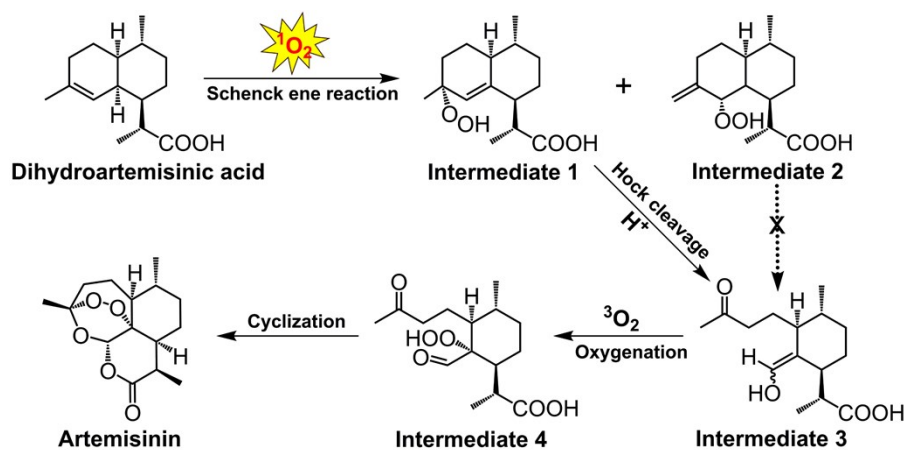


Fig. S14. Reaction path of photocatalytic oxidation of dihydroartemisinic acid to artemisinin.

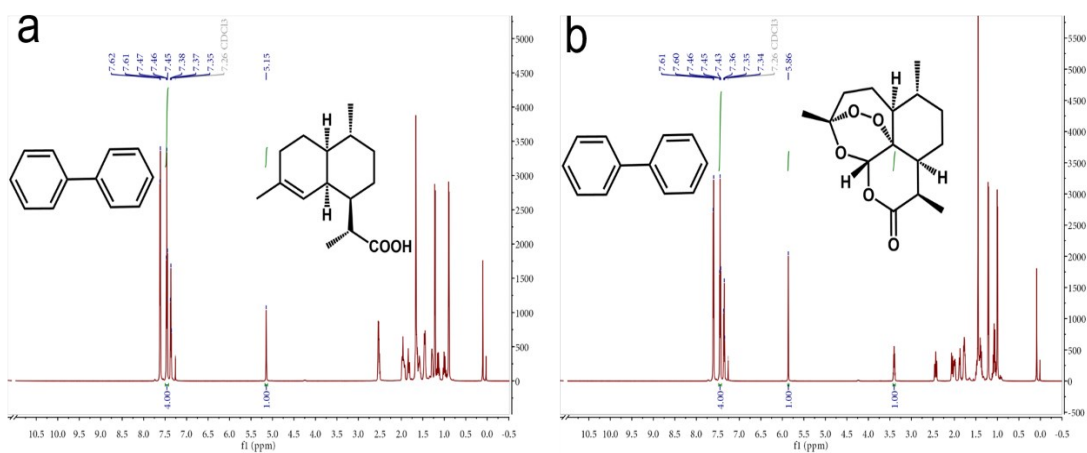


Fig. S15. ^1H NMR spectra of commercial dihydroartemisinic acid (a) and artemisinin (b) (Reaction conversions and yields were monitored by ^1H NMR using biphenyl as an internal standard.).

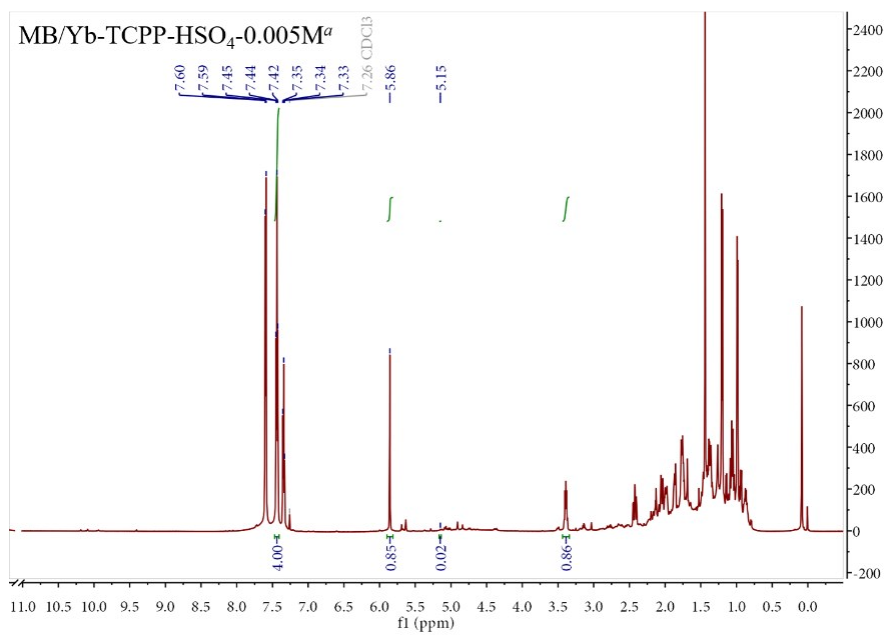


Fig. S16. ¹H NMR spectrum of product catalyzed by MB/Yb-TCPP-HSO₄-0.005M^a.

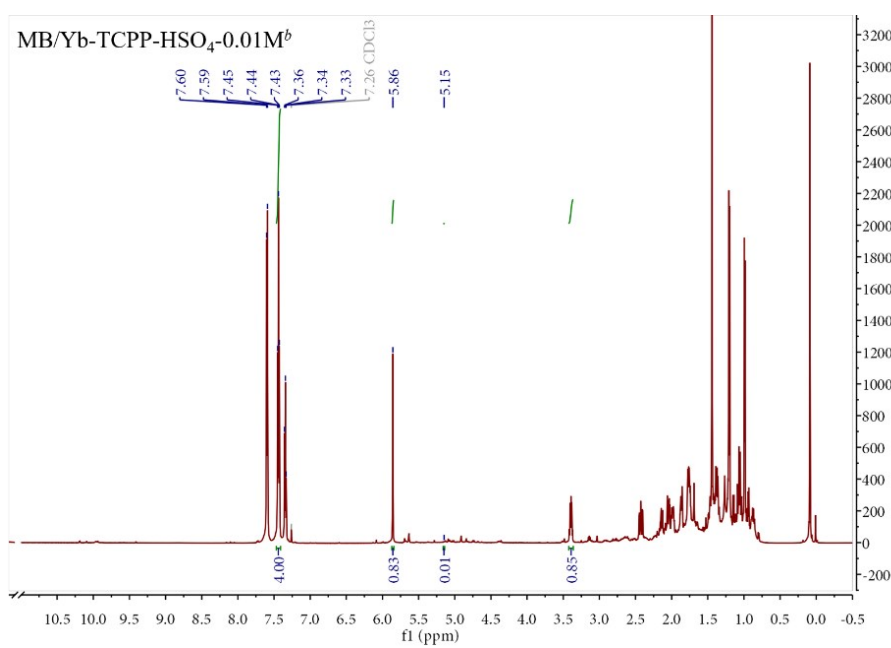


Fig. S17. ¹H NMR spectrum of product catalyzed by MB/Yb-TCPP-HSO₄-0.01M^b.

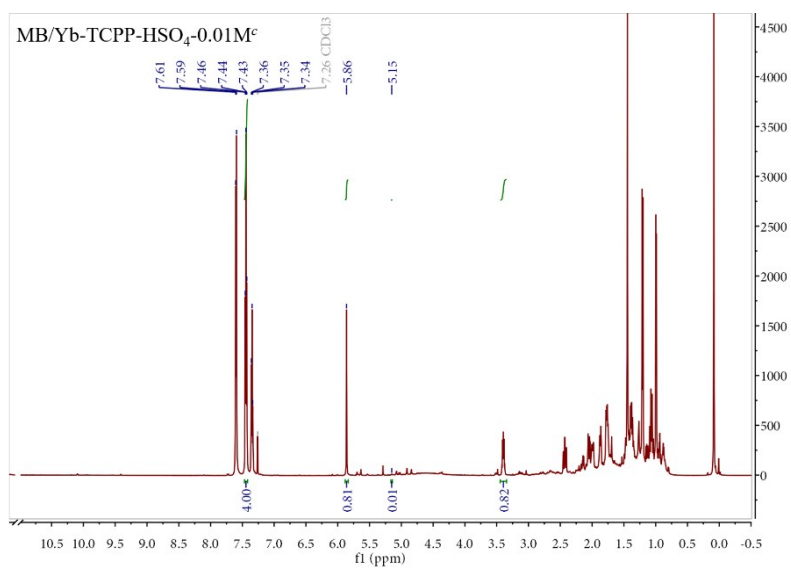


Fig. S18. ^1H NMR spectrum of product catalyzed by MB/Yb-TCPP- $\text{HSO}_4\text{-}0.01\text{M}^c$.

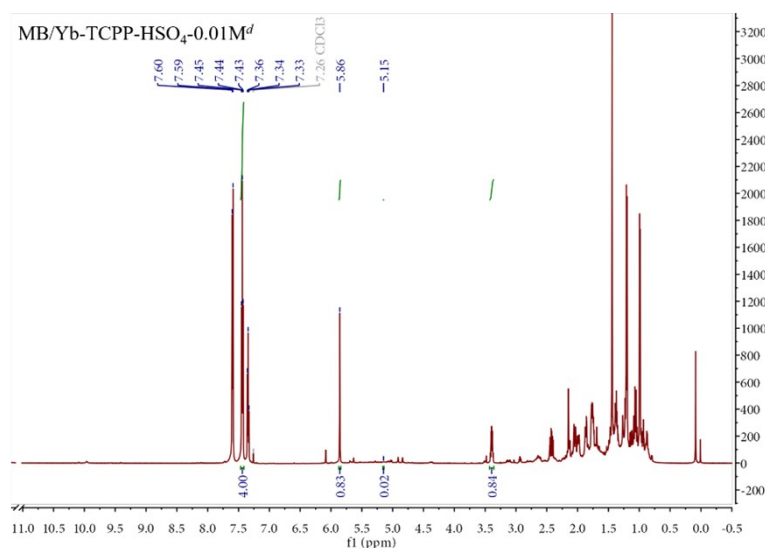


Fig. S19. ^1H NMR spectrum of product catalyzed by MB/Yb-TCPP- $\text{HSO}_4\text{-}0.01\text{M}^d$.

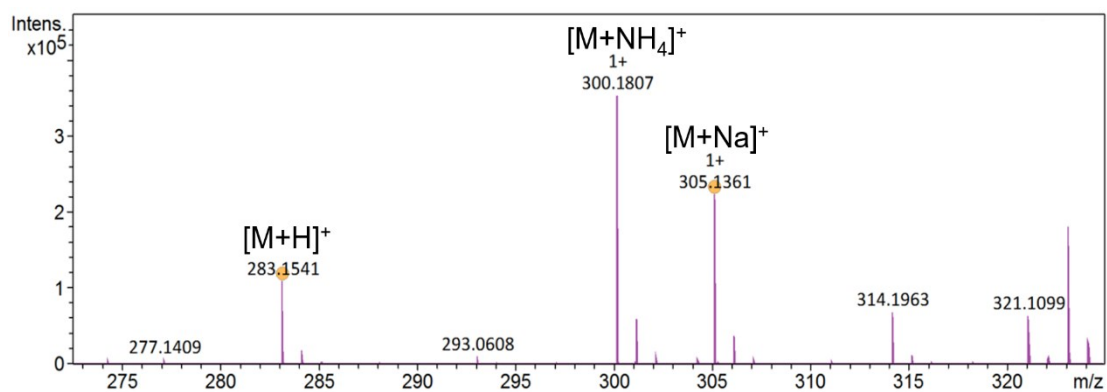


Fig. S20 The mass spectrum of product under positive ion mode. The m/z at 283.1541, 300.1807, 305.1361 were assigned to $[\text{M}+\text{H}]^+$, $[\text{M}+\text{NH}_4]^+$, $[\text{M}+\text{Na}]^+$, respectively, further demonstrating the product is artemisinin ($M_w = 282.15$).

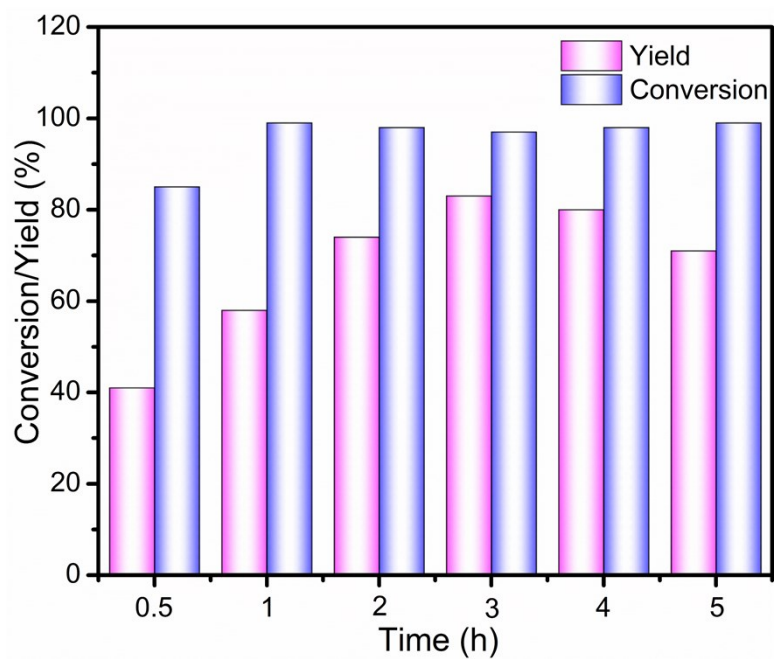


Fig. S21. Optimization of reaction time for photocatalytic synthesis of artemisinin.

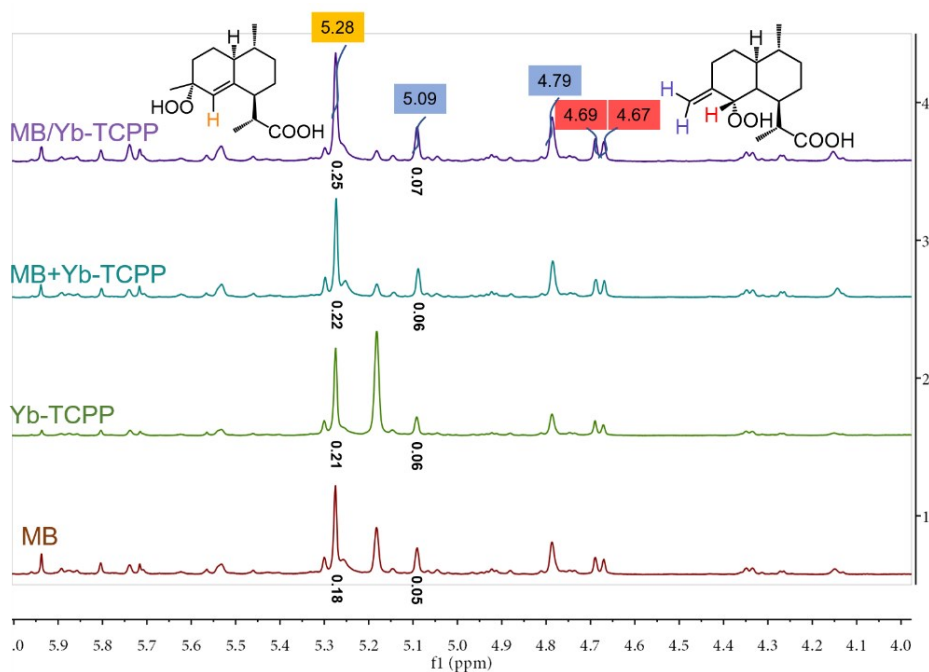


Fig. S22. The ^1H NMR of intermediate 1 and 2 in acetone- d_6 after photooxidation of dihydroartemisinic acid for 1 hour.

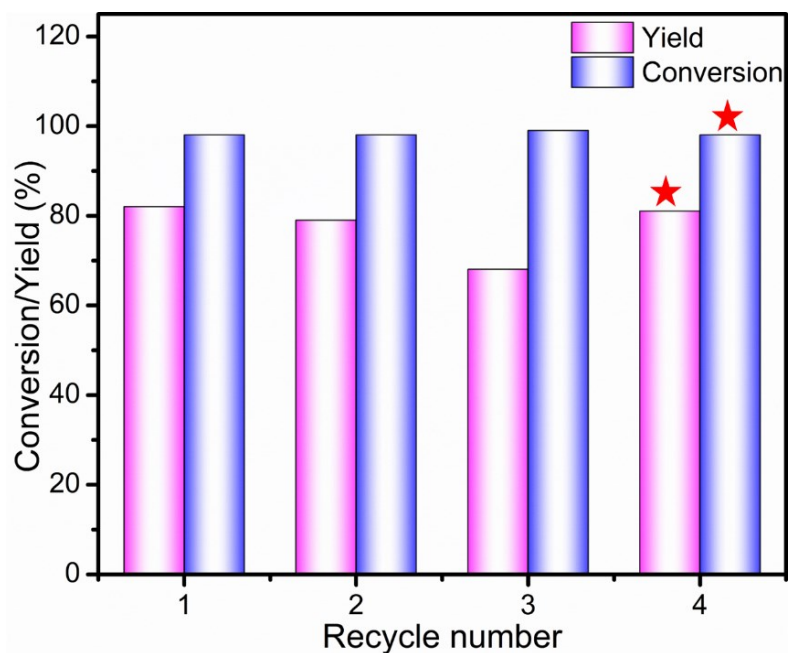


Fig. S23. Recyclability of 2D MB/Yb-TCPP- HSO_4 -0.005M- H_2SO_4 nanosheets for photocatalytic synthesis of artemisinin from dihydroartemisinic acid (★: the yield and conversion were recovered after acid treatment again).

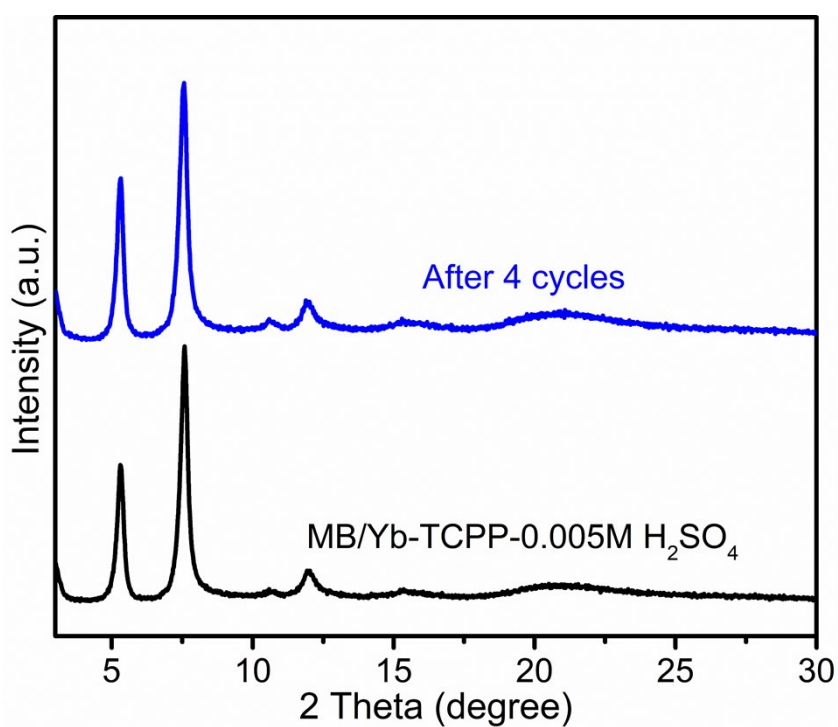


Fig. S24. PXRD patterns of 2D MB/Yb-TCPP-0.005M- H_2SO_4 nanosheets before (black curve) and after four cycles (blue curve) of catalytic reactions.

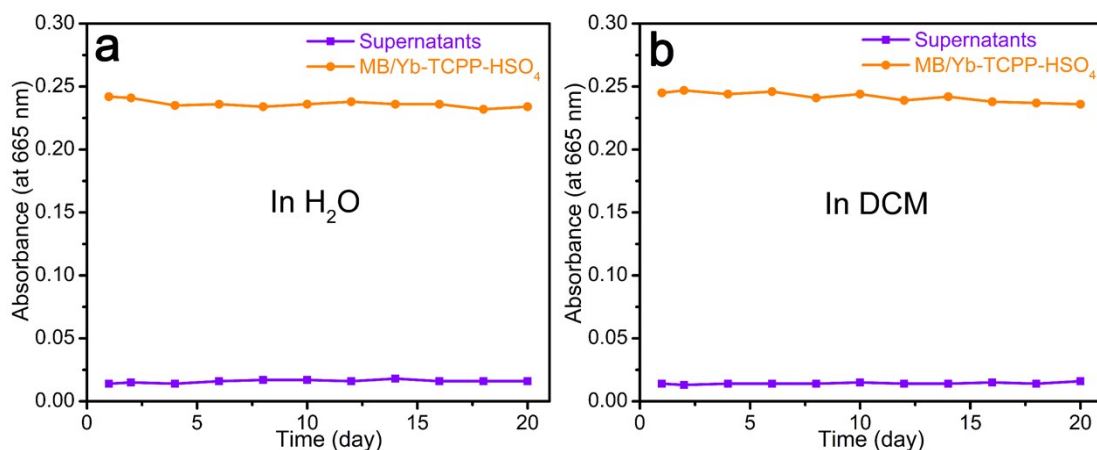


Fig. S25. The leaching test of 2D MB/Yb-TCPP-HSO₄ nanosheets in (a) H₂O and (b) dichloromethane (DCM).

Table S1. The pH of the washing solution of the as-constructed 2D ALHSs before and after acidification.

Compound	pH
MB/Yb-TCPP-SO ₄	7.86
MB/Yb-TCPP-HSO ₄ ^a	2.19
MB/Yb-TCPP-HSO ₄ ^b	2.24
MB/Yb-TCPP-HSO ₄ ^c	2.26
MB/Yb-TCPP-HSO ₄ ^d	2.23

^a treatment with 0.005M H₂SO₄; ^b treatment with 0.01M HNO₃; ^c treatment with 0.01M HCl; ^d treatment with 0.01M TFA.

Table S2. The ¹O₂ quantum yield of different photocatalytic system calculated by using RB as a standard photosensitizer in ethanol.

Compound	PL peak areas (I)	¹ O ₂ quantum yield (Φ)
RB	138408	0.86
MB	88534	0.55
Yb-TCPP	99555	0.62
MB+Yb-TCPP	101609	0.63
MB/Yb-TCPP-SO ₄	106611	0.66
MB/Yb-TCPP-HSO ₄	105234	0.65

Calculation formula: $\Phi_{\text{Photocatalyst}} = \Phi_{\text{RB}} (I_{\text{Photocatalyst}}/I_{\text{RB}})$

Reference:

- Z. W. Jiang, Y. C. Zou, T. T. Zhao, S. J. Zhen, Y. F. Li and C. Z. Huang, *Angew. Chem. Int. Ed.*, 2020, **59**, 3300-3306.

- 2 J. Jiang, F. Gandara, Y. B. Zhang, K. Na, O. M. Yaghi and W. G. Klemperer, *J. Am. Chem. Soc.*, 2014, **136**, 12844-12847.
- 3 C. A. Trickett, T. M. Osborn Popp, J. Su, C. Yan, J. Weisberg, A. Huq, P. Urban, J. Jiang, M. J. Kalmutzki, Q. Liu, J. Baek, M. P. Head-Gordon, G. A. Somorjai, J. A. Reimer and O. M. Yaghi, *Nat. Chem.*, 2018, **11**, 170-176.
- 4 A. Zheng, S. J. Huang, S. B. Liu and F. Deng, *Phys. Chem. Chem. Phys.*, 2011, **13**, 14889-14901.
- 5 A. Zheng, H. Zhang, X. Lu, S.-B. Liu and F. Deng, *J. Phys. Chem. B*, 2008, **112**, 4496-4505.
- 6 L. Feng, Y. Wang, S. Yuan, K.-Y. Wang, J.-L. Li, G. S. Day, D. Qiu, L. Cheng, W.-M. Chen, S. T. Madrahimov and H.-C. Zhou, *ACS Catal.*, 2019, **9**, 5111-5118.
- 7 Y. Wang, L. Feng, J. Pang, J. Li, N. Huang, G. S. Day, L. Cheng, H. F. Drake, Y. Wang, C. Lollar, J. Qin, Z. Gu, T. Lu, S. Yuan and H. C. Zhou, *Adv. Sci.*, 2019, **6**, 1802059.